Prospecting alpine permafrost with Spectral Induced Polarization in different geomorphological landforms

D2651 | EGU2020-10131

Theresa Maierhofer, Timea Katona, Christin Hilbich, Christian Hauck, Adrian Flores-Orozco

EGU General Assembly 2020

Introduction and State of the Art

- Climate change – permafrost degradation → monitoring of the ice content has become an essential task also in the European Alps
- Permafrost measurements
  - Borehole temperatures (only point information)
  - Geophysical measurements: Electrical Resistivity Tomography (ERT), Refraction Seismic Tomography (RST) – standard measurement techniques in permafrost

Refraction Seismic Tomography

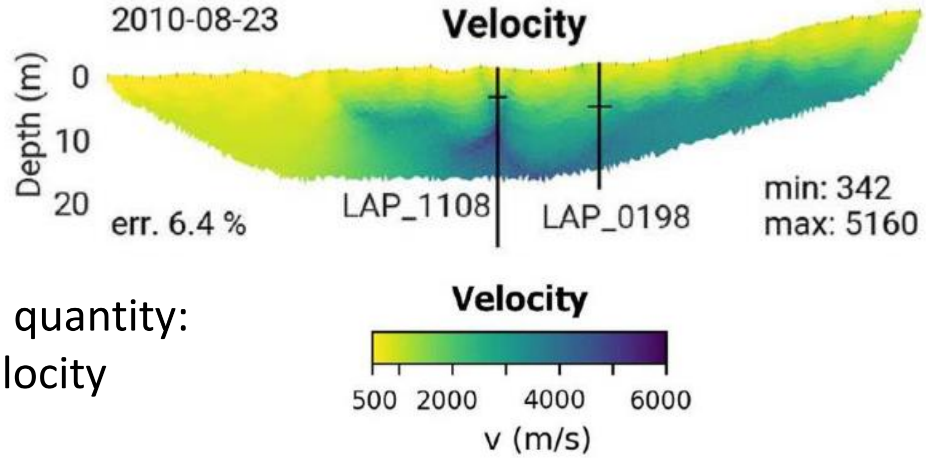

Measured quantity:
P-wave velocity

Electrical Resistivity Tomography

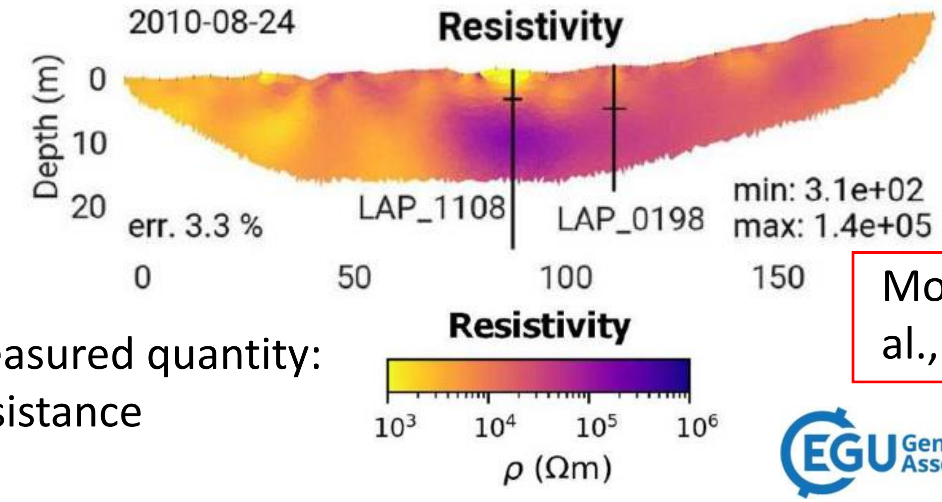

Measured quantity:
Resistance

Mollaret et al., 2020

Introduction and State of the Art

- Joint inversion of ERT-RST to estimate the volumetric fractions of liquid water, ice and air and rock matrix – Coline Mollaret and Florian Wagner
  - Joint inversion contributes to improved quantification of water ice and air

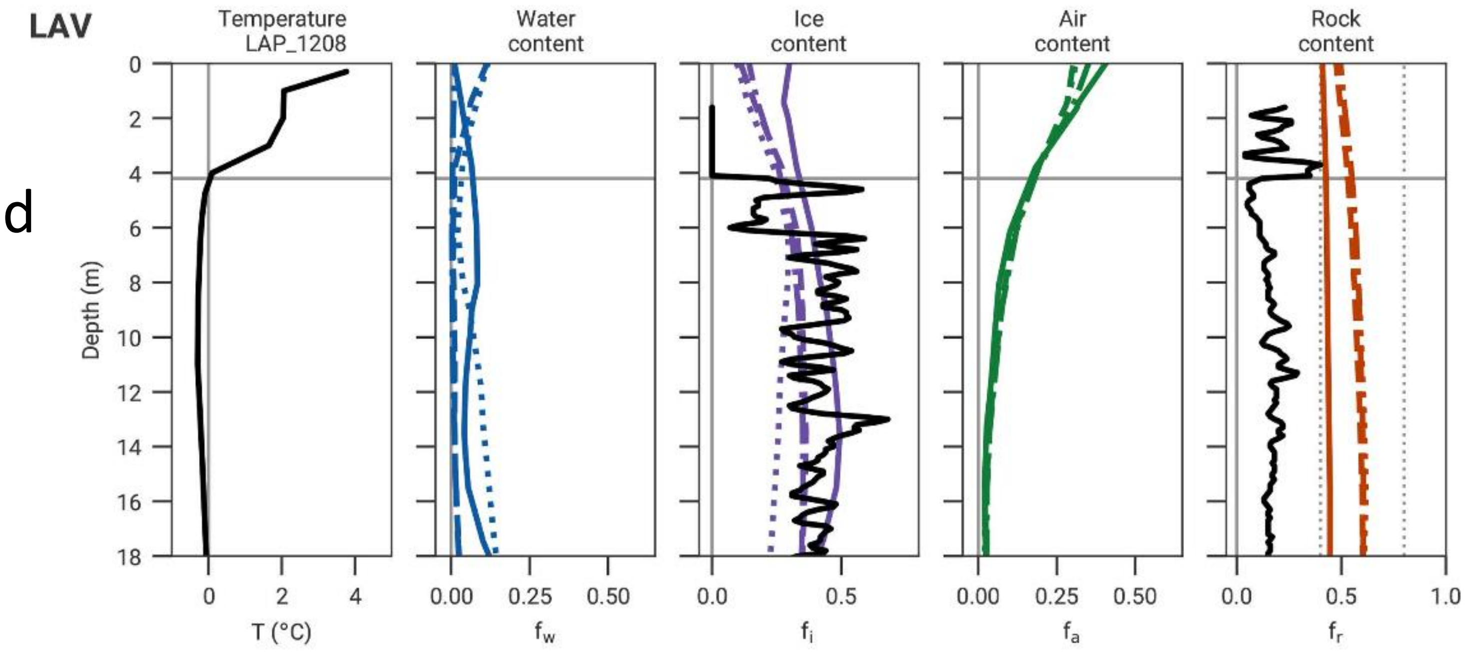

Mollaret et al., 2020

- But still some remaining ambuiguities between ice and rock matrix

  Since resistivity and P-wave velocity of ice and rock are often too similar to be distinguished by ERT and RST alone – additional information is needed

  Therefore we propose and test the applicability of a new method: Induced Polarization (IP) – Complex Resistivity Tomography

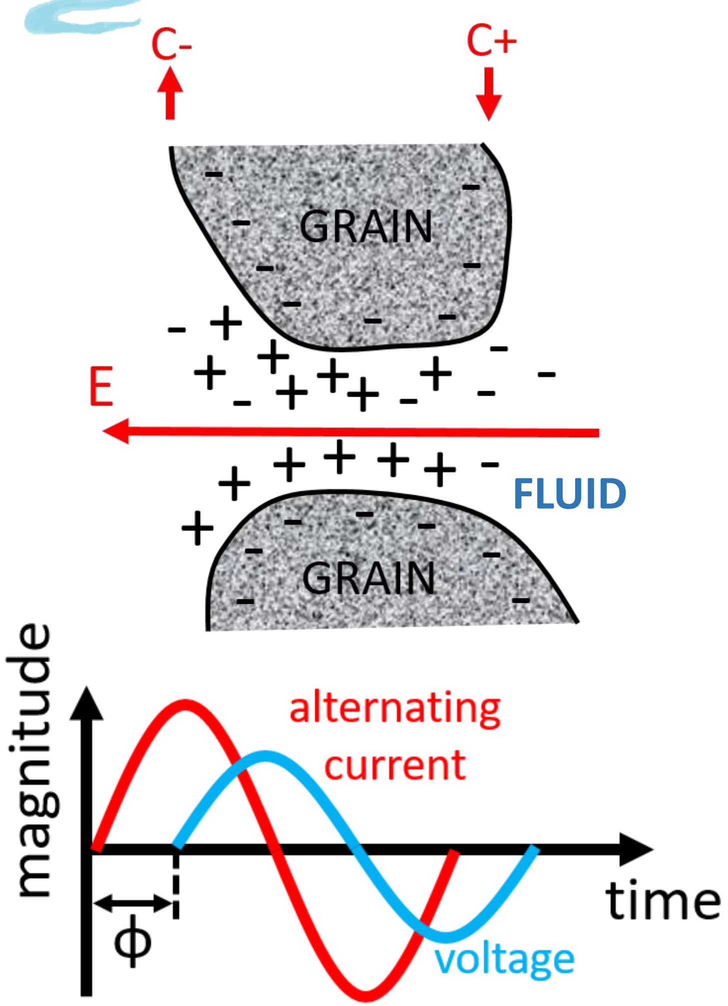

$\rho^* = \rho' + i\rho'' = \log|\rho| + i\phi$

Induced Polarization

In Frequency Domain:

- An alternating current is injected at low frequencies (commonly below 1 kHz on the field and below 50 kHz in the laboratory)
- In polarizable materials we observe a phase-shift (ϕ) between the injected current and measured voltage
- Complex electrical resistivity/conductivity expressed in terms of the real and imaginary components or by its magnitude (ratio voltage/current) and phase (shift between voltage/current)
  - Real part: Conduction mechanisms
  - Imaginary part: Polarization processes

Spectral Induced Polarization

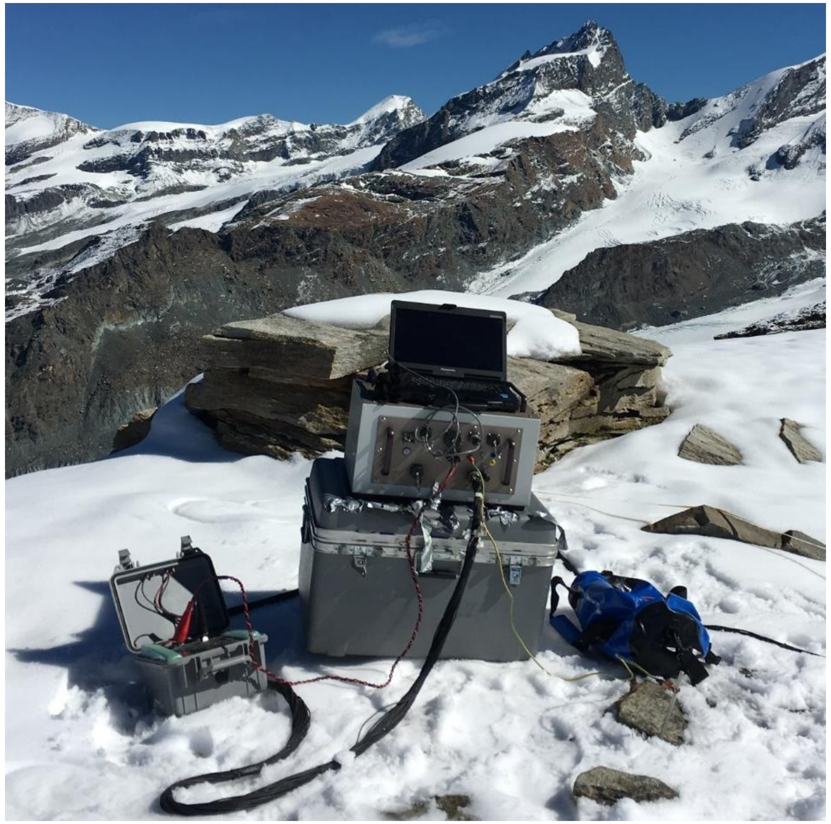

DAS-1 (TDIP and FDIP measurements at frequencies between 0.01-225 Hz)

- Repetition of the measurement at different frequencies (0.01-1000 Hz)
- To gain information about the frequency-dependence of the electrical properties (resistivity and IP)
  - Fast polarization effects – e.g., small grains – take place at high frequencies (small pulse lengths)
  - Slow polarization effects – e.g., big grains – take place at low frequencies (high pulse lengths)

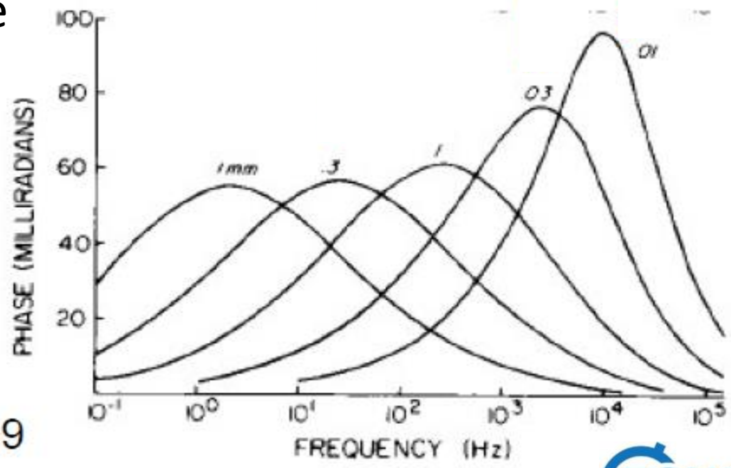

Wong, Geophysics 1979

Polarization mechanisms in permafrost environments

The inversion of the data allows us to resolve for the electrical resistivity (ρ [Ωm]) and the phase (ϕ [mrad]) or the real (ρ’ [Ωm]) and imaginary (ρ’’ [Ωm]) component of the complex resistivity of subsurface materials

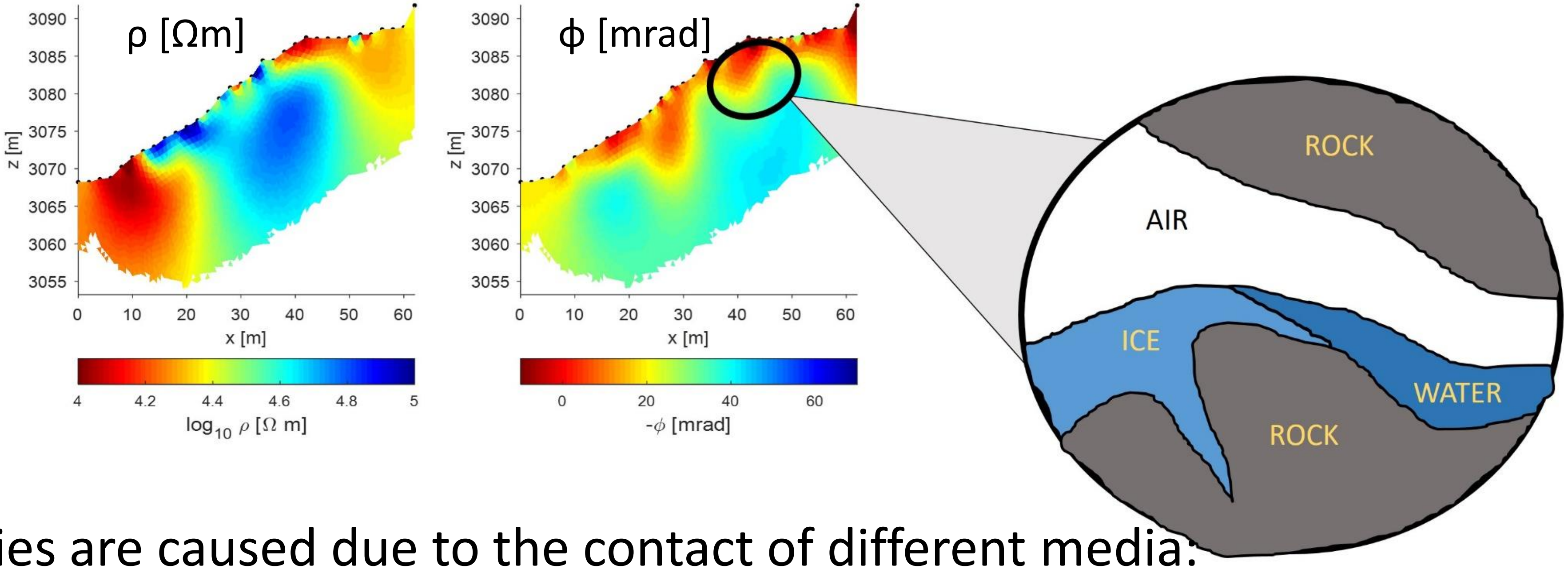

Hypotheses: IP anomalies are caused due to the contact of different media:

?

air/rock	air/water	air/ice	rock/ice	rock/water	water/ice
no IP effect	no IP effect	no IP effect	no IP effect	medium IP effect	high IP effect

Applicability of IP method for Alpine Permafrost

Challenges of collecting reliable SIP data at the field-scale?

- Heavy equipment, high electrode contact resistances (sometimes >100 kilo Ohms) because of blocky surface → weak signal strength, low current injections (as for ERT surveys)
- Additional challenges for SIP: polarization of the electrodes, anthropogenic structures (high metal content), electromagnetic coupling (cross-talking with the cables, induction effects in the ground)
- How much can we trust in our data?

To enhance data quality of field SIP measurements

- Tests of different measuremt protocols and cable layouts
- Identification and quantification of errors in the data

Electromagnetic coupling

- Main limitation of field frequency-domain SIP imaging: contamination of the data due to parasitic electromagnetic fields (especially at frequencies above 10 Hz)
- EM coupling caused by inductive or capacitive sources
  - Cross talking between cables used for current injection and voltage measurements, induction of EM fields → tests of different cable-setups for an improvement in data quality

Separation of current and potential cables

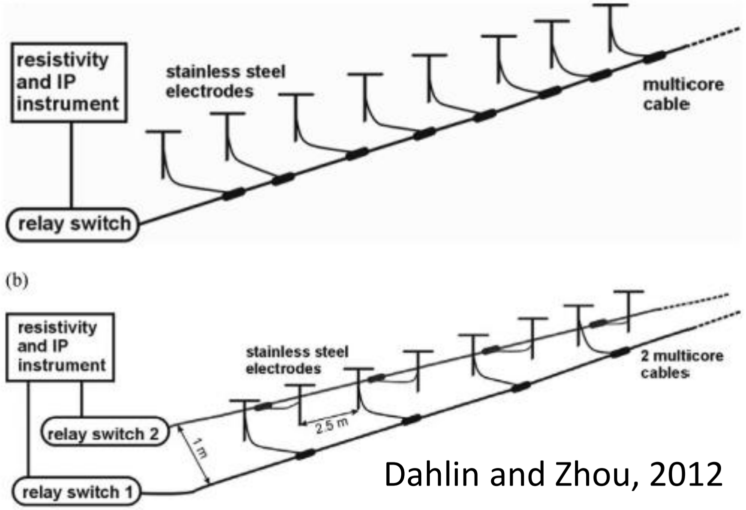

Dahlin and Zhou, 2012

Coaxial cables (shielded cables)

Removal of outliers and quantification of data error via normal and reciprocal analysis

- Normal and reciprocal (N&R) measurements refer to a repetition of the measurement by interchanging current and potential dipoles – used to identify outliers, quantify the data quality and the data error, filtering approach: Flores-Orozco, 2019

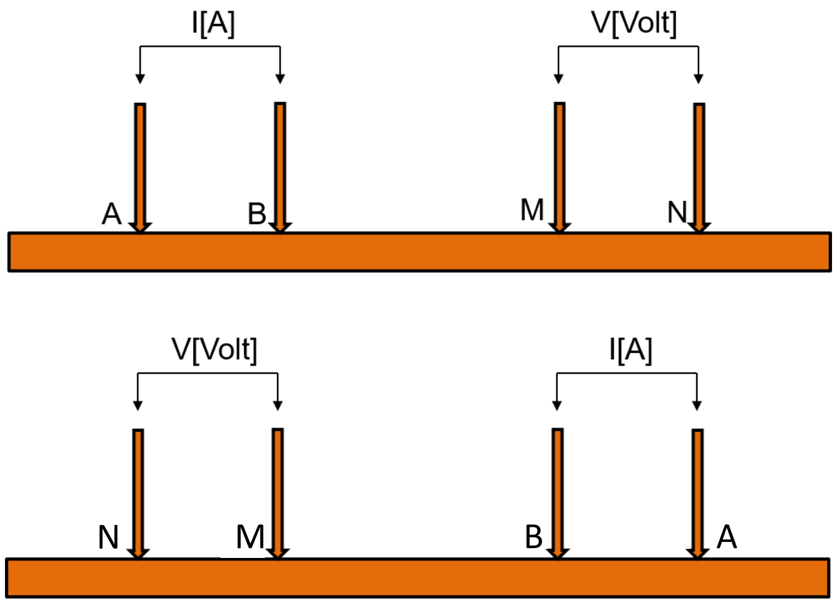

Pseudosection of apparent resistivity and phase

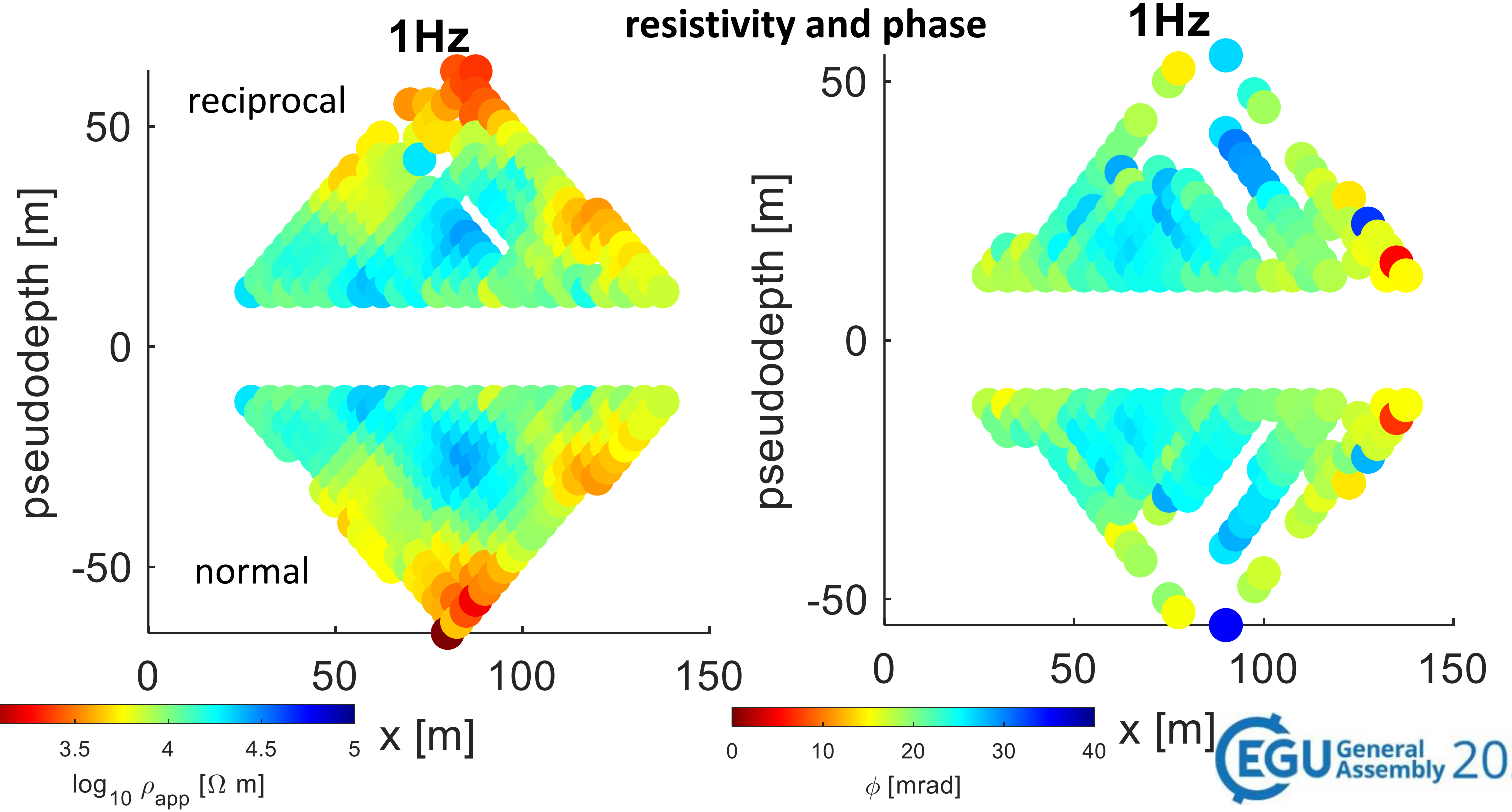

Extensive field tests in LAPIRES, Valais Alps, Swiss Alps

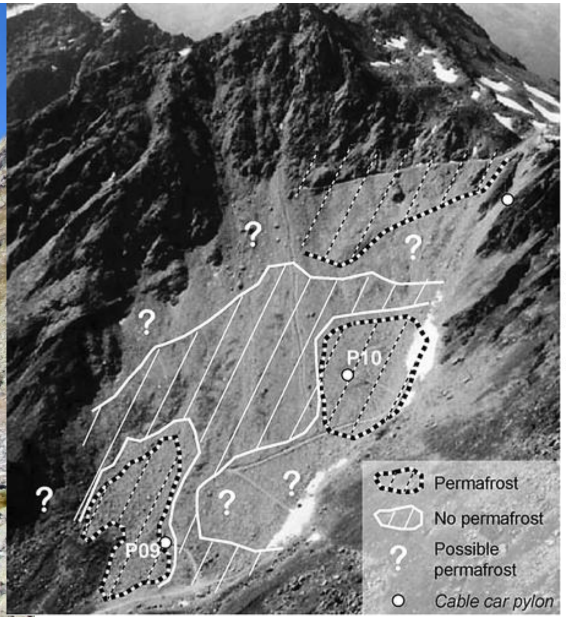

Delaloye, 2004

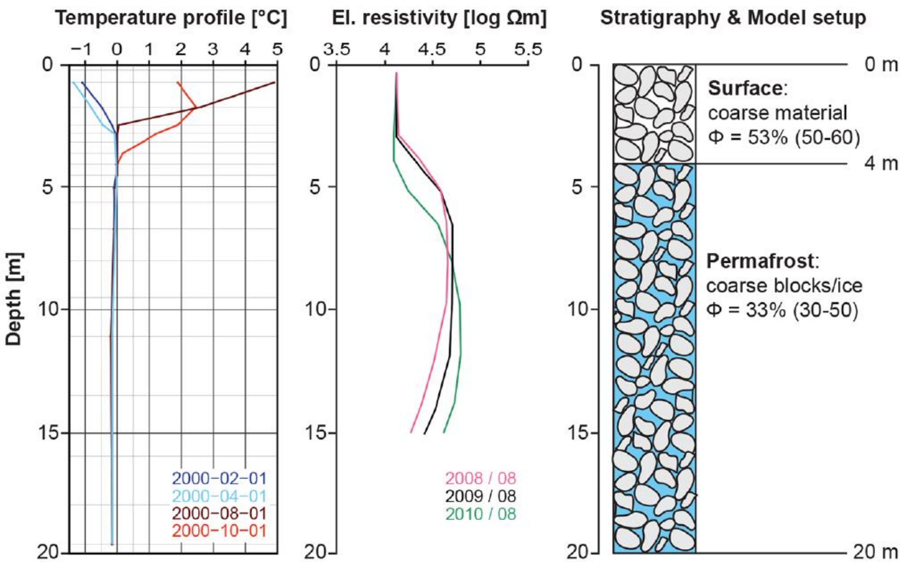

Staub et al. 2015

- large NE oriented talus slope (~500m width)
- composition of the talus slope defined from four boreholes, geophysical measurements and ground temperature records
- metamorphic blocks (mainly gneiss and schists)
- temperate permafrost close to the melting point (internal air circulation “chimney effect”)
- ice rich permafrost body (15m), 4 - 5.5m thick active layer

Lapires - applicability of IP method for Alpine Permafrost

Extensive field tests in LAPIRES, Valais Alps, Swiss Alps

Analysis: Christian Scapozza

We chose this site due to:

- the spatial variable, but clearly defined ground ice occurrences
- Comparatively high ice content
- 4 boreholes
- Extensive additional geophysical data present
- Medium size blocks at the surface (average for permafrost)
- All contacts between different media (air/ice, rock/ice, water/ice etc.) potentially present

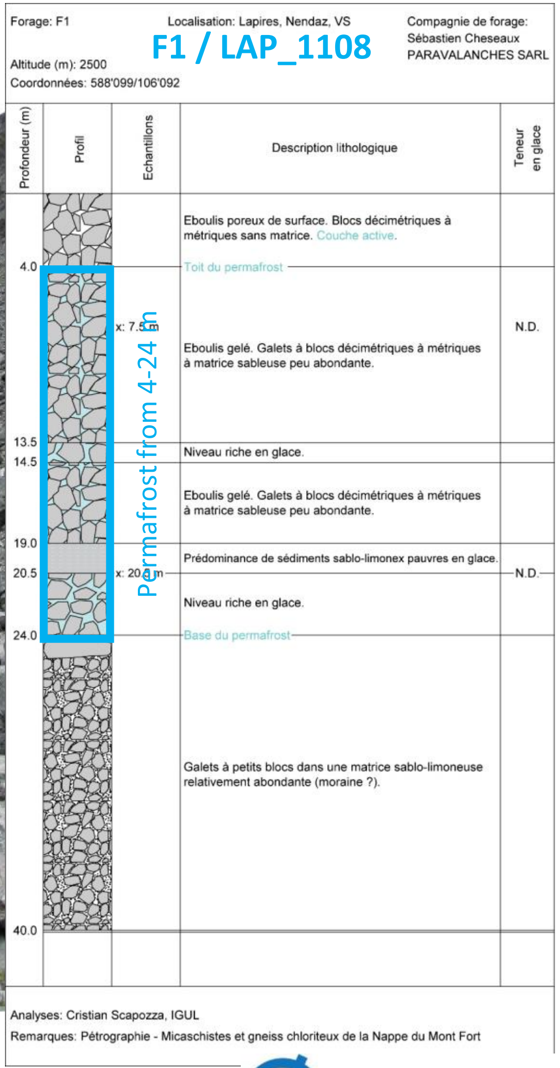

Additional qualitative or spatial information from IP response

Mapping of complex resistivity (Dipole Dipole: 0.5-225Hz, Multiple Gradient: 0.1-225Hz)

- Profiles P2, P3, P4, P5 with 10m electrode separation
- Profile P1 with 5m electrode separation
- ERT monitoring profile with 3m electrode separation

- The blue polygon marks permafrost occurence defined by previous studies (Staub et al., 2015)

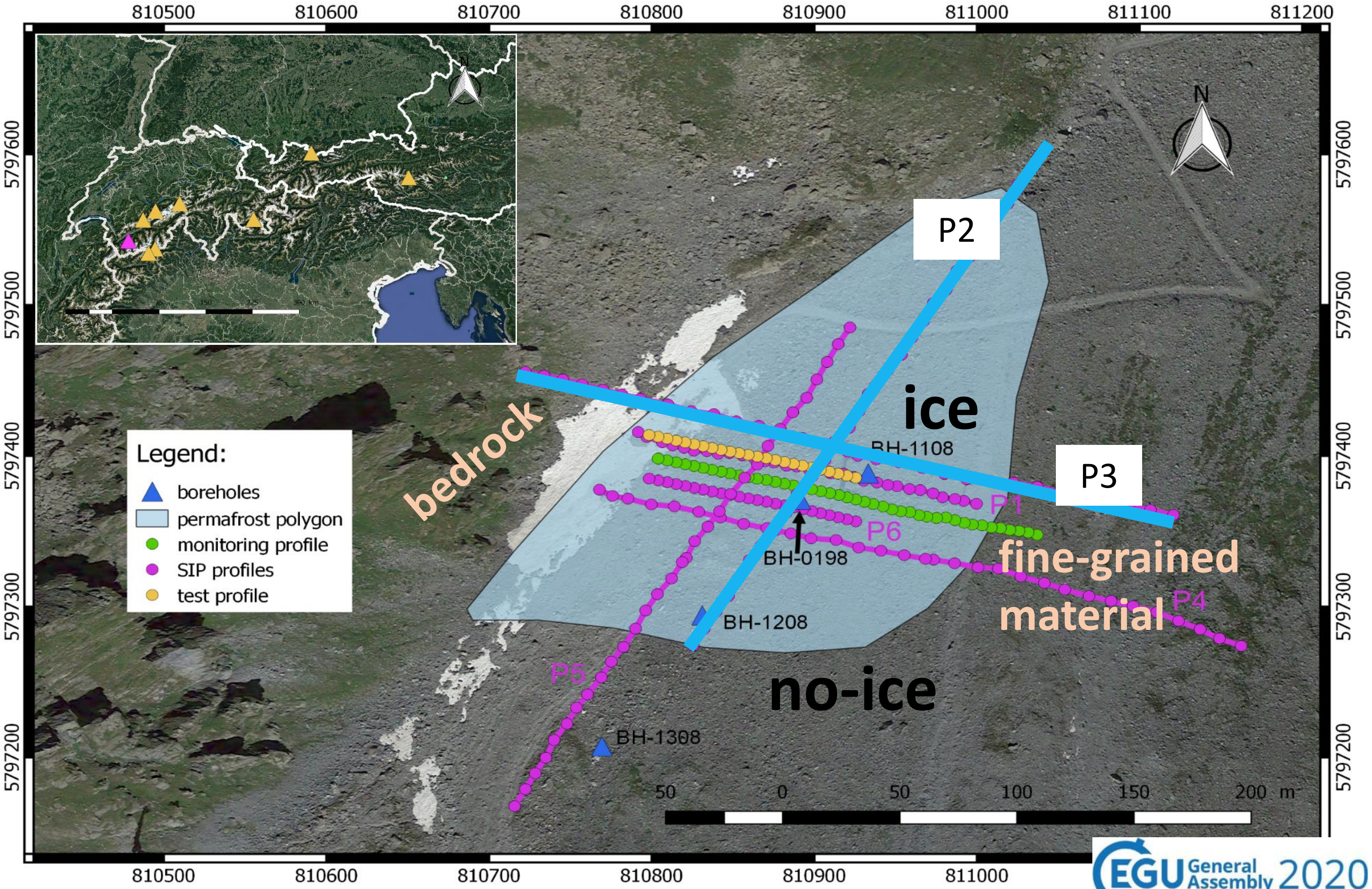

Additional qualitative or spatial information from IP response

- Are we able to see a difference in our spectral induced polarization data for ice-rich areas and areas without ice?
  - Therefore, we first had a look into our raw data (the electrical impedance) → apparent resistivty and phase for different frequencies and observed the lateral change of the quantities

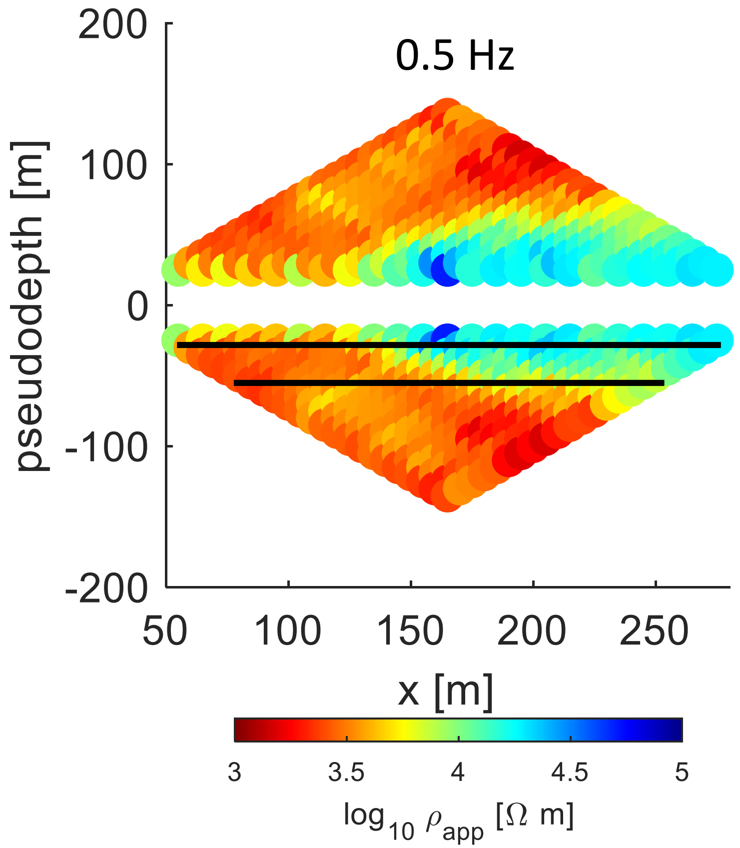

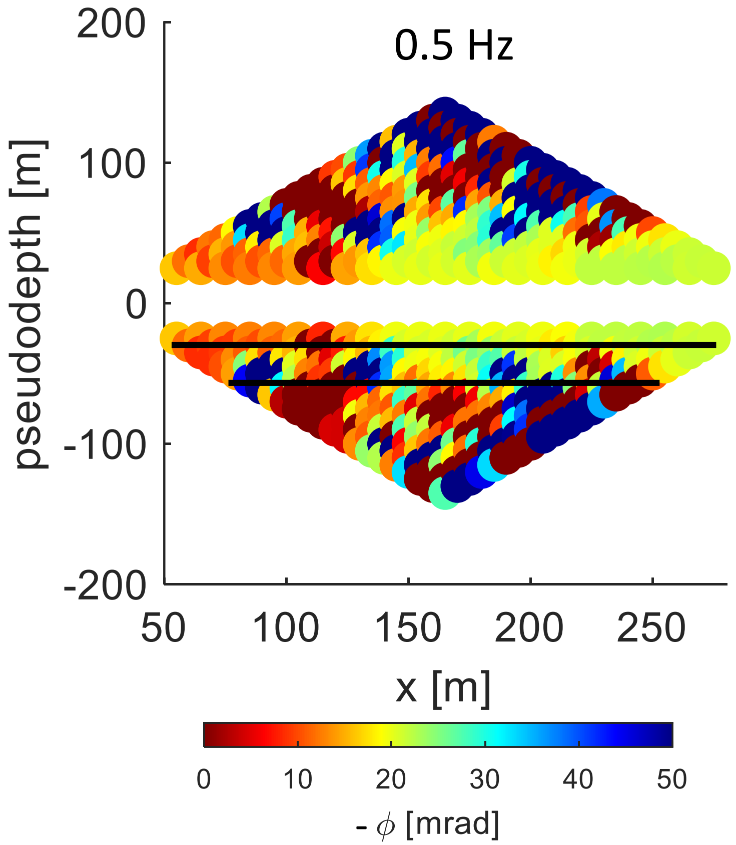

Additional qualitative or spatial information from IP response

Lateral change in apparent resistivity

collected along profile P2 for selected dipoles

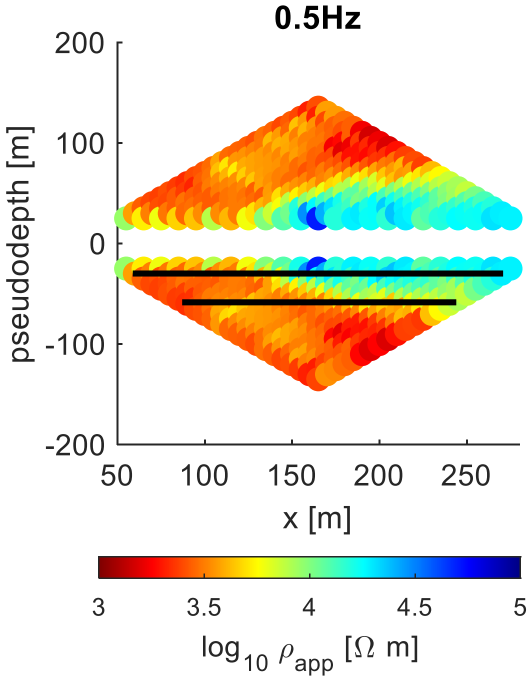

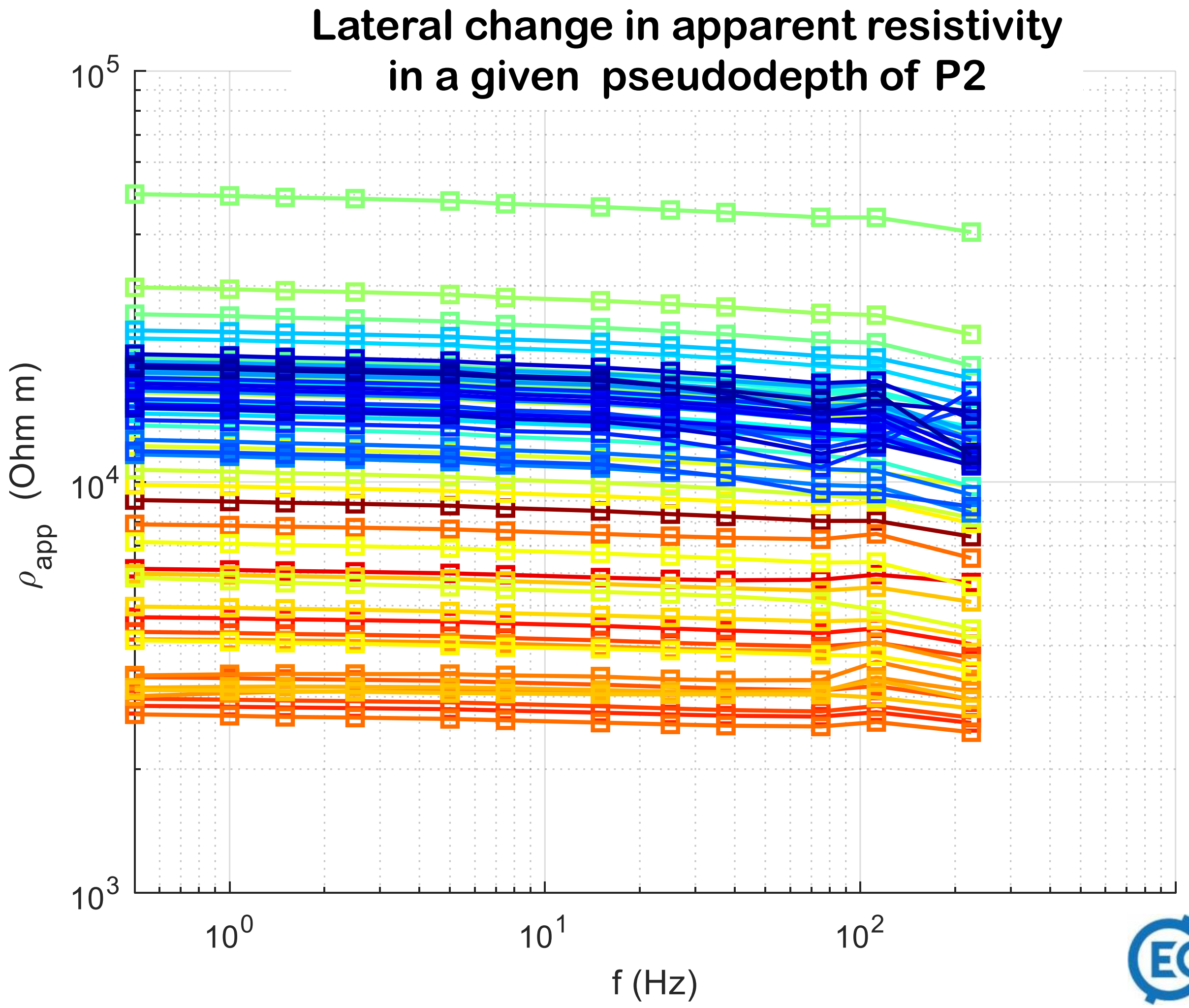

→ High apparent resistivity values for all frequencies for the ice-rich part of the profiles are observed

→ No frequency dependence

Additional qualitative or spatial information from IP response

Lateral change in apparent phase
collected along profile P2 for selected dipoles

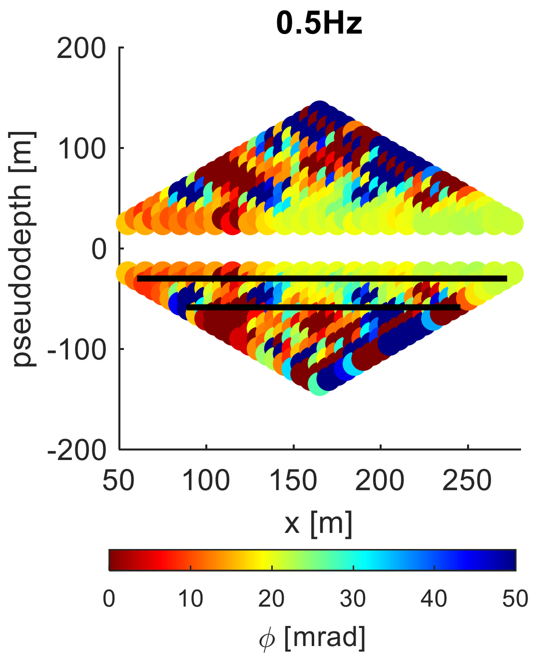

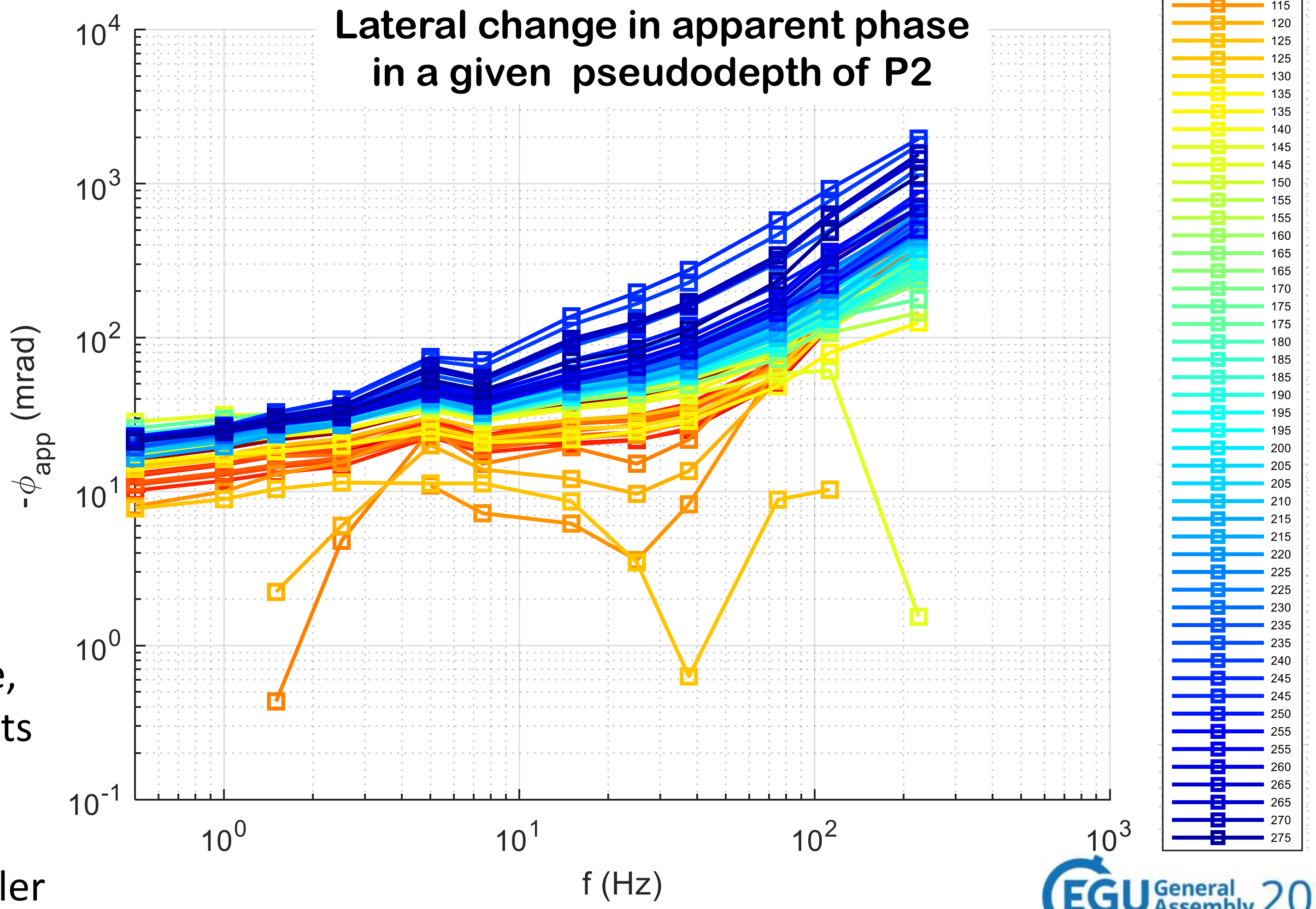

→ For ice-rich parts: higher polarization response, constant increase of polarization measurements from 7.5 Hz

→ For parts with no ice, lower polarization response, the increase with frequency is smaller

Additional qualitative or spatial information from IP response

- Are we able to see a difference in our spectral induced polarization data for ice-rich areas and areas without ice?

Inversion results at different frequencies - imaginary part of complex resistivity

real part of complex resistivity

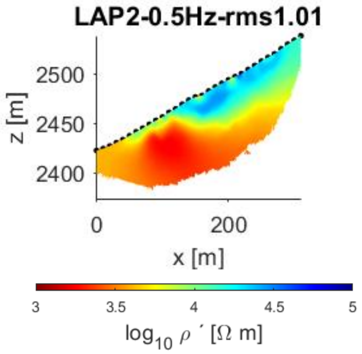

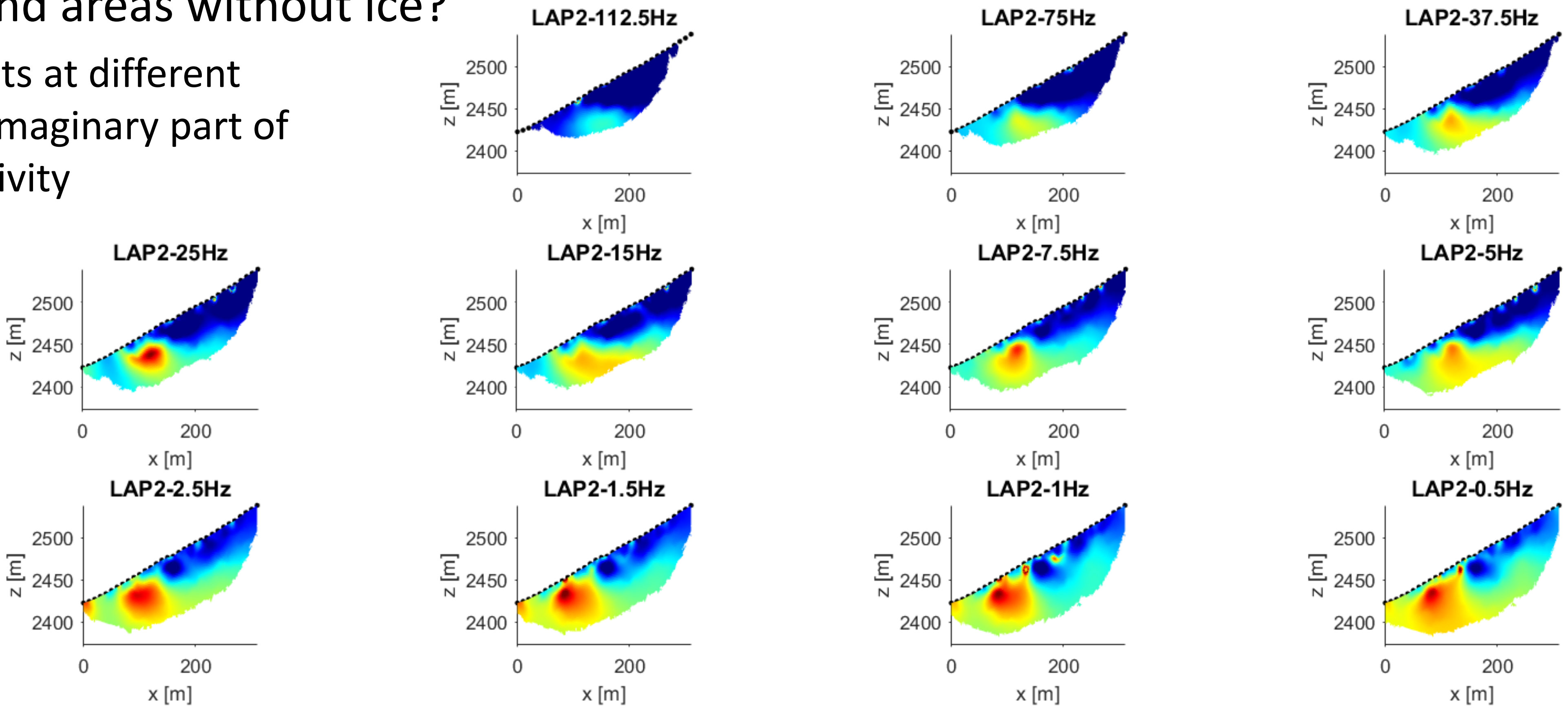

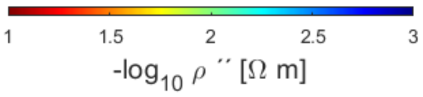

Observations:

- Frequency dependence in polarization response
- Lateral change in polarization response
- Change in depth

Additional qualitative or spatial information from IP response

- Extracted complex resistivity values in ice-rich part and part with no ice

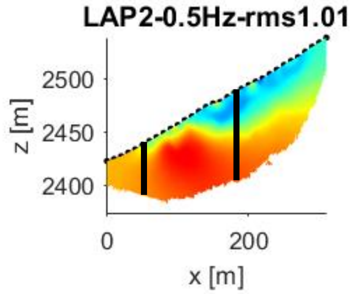

NO ICE

ICE

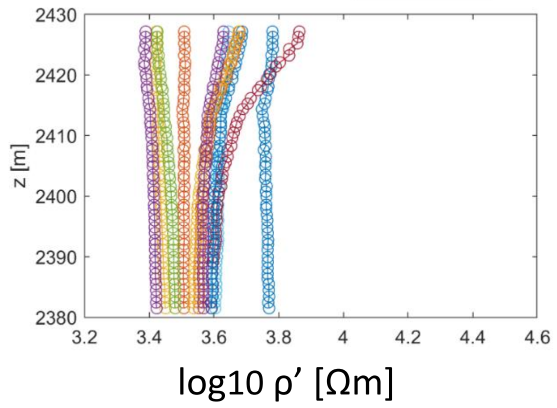

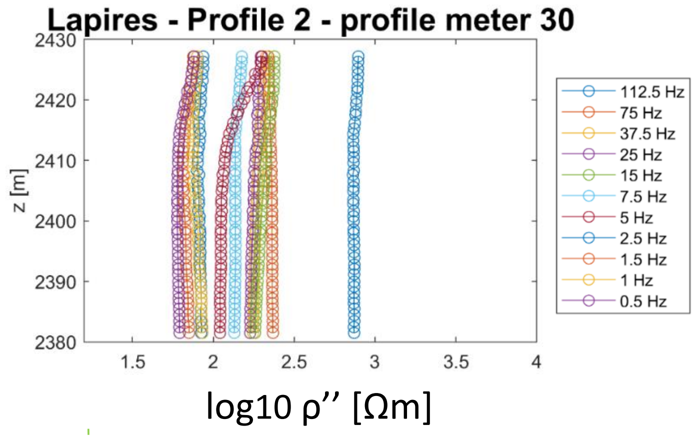

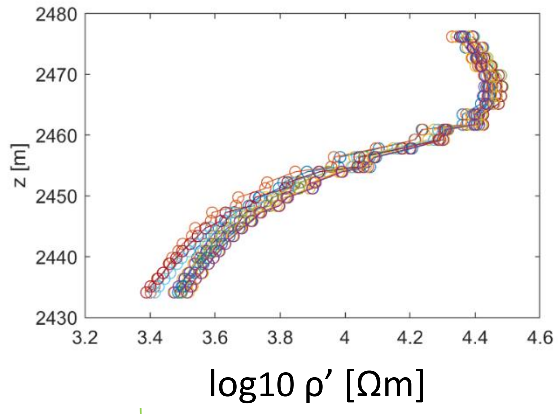

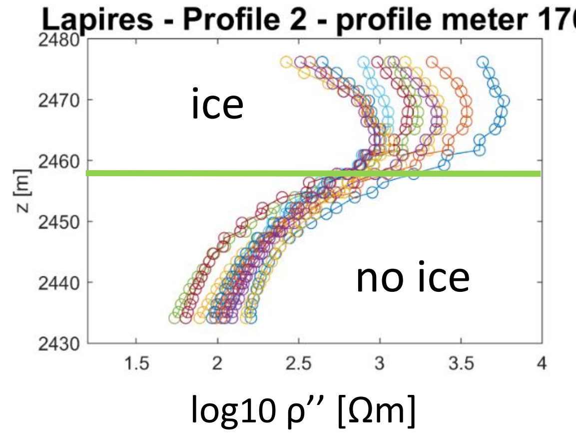

- Values of the real part of the complex resistivity between 3.4-3.8 Ωm in logarithmic scale
- Values of imaginary part of the complex resistivity between 1.7-2.5 Ωm in logarithmic scale
- no change in depth

- Values of the real part of the complex resistivity between 4.2-4.6 Ωm in logarithmic scale
- Values of imaginary part of the complex reesistivity between 2.5-3.8 Ωm in logarithmic scale
- Change in depth: frequency dependence in imaginary part more pronounced for first 20 metres than for deeper parts

IP response at different permafrost sites

We tested the method at 8 different permafrost sites within the Swiss, Italian and Austrian Alps covering different ice contents and contacts between materials (e.g. wet, dry, coarse blocky, bedrock sites etc). Here we show 3 additional sites.

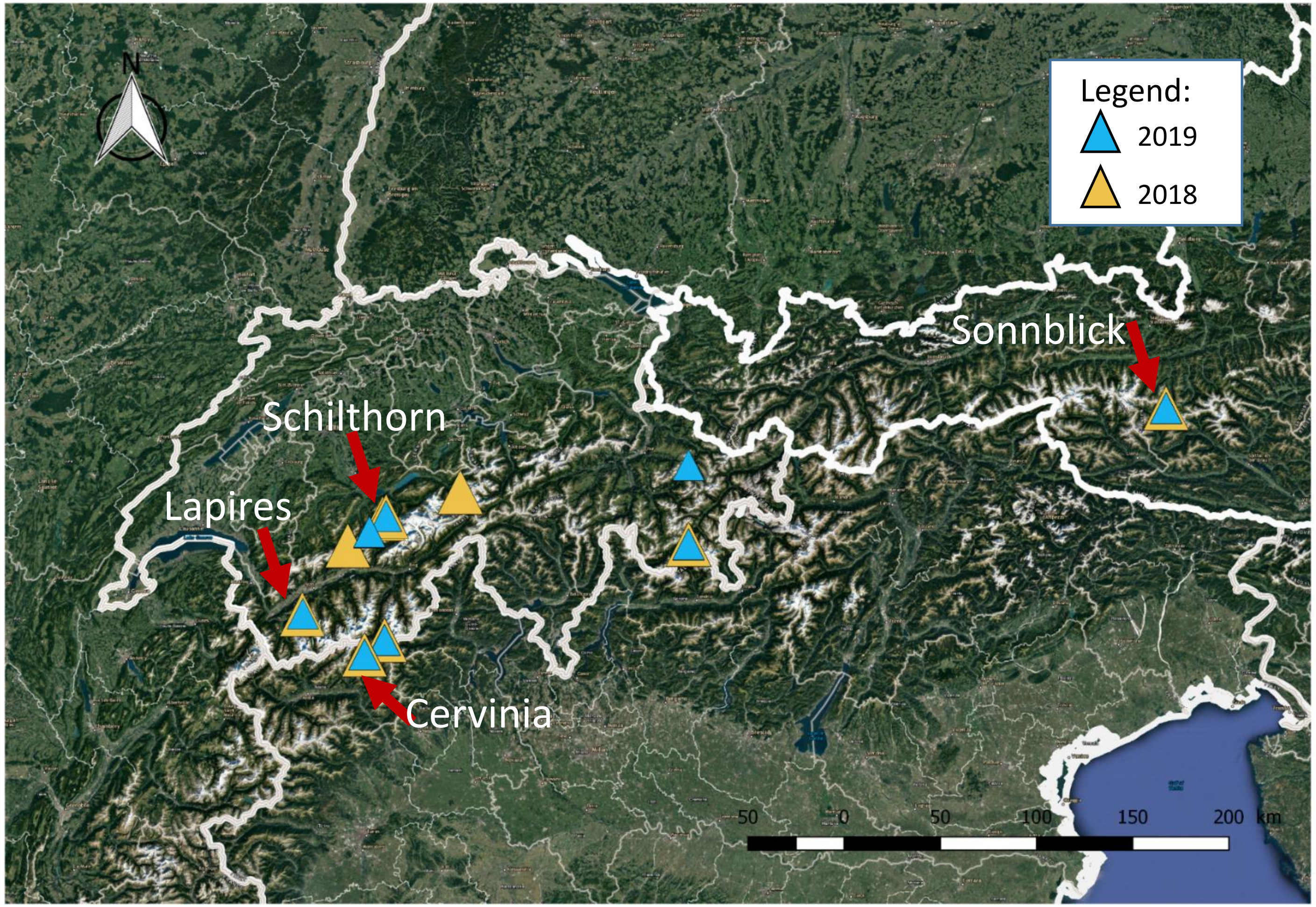

Measurements 2018:

- Lapires
- Cervinia
- Schilthorn
- Stockhorn
- Murtel
- Sonnblick
- Hundshore
- Tierhöri

Measurements 2019:

- Lapires
- Cervinia
- Schilthorn
- Stockhorn
- Murtel
- Sonnblick
- Totalphorn
- Spitze Stei/Oeschinensee

Sonnblick, Austria

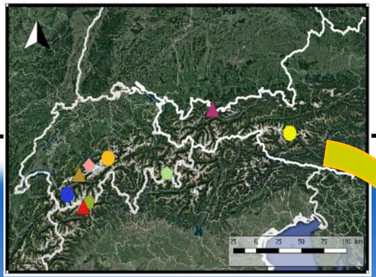

- Sonnblick – 3106m
- Austrian Central Alps
- Mean annual air temperatures ~-4.7°C
- Geology of the Tauernfenster (mainly granite gneiss with potash feldspar)
- 3 boreholes of 20m depth
- ALT around 1-2m
- What was the aim of the study: Additional information from SIP?
- Additional information for validation: Refraction Seismic Tomography, Electromagnetic measurements, GPR

IP response measured at Sonnblick, Austria

- Complex resistivity data collected along a profile in vicinity of the 3 boreholes

real part of complex resistivity

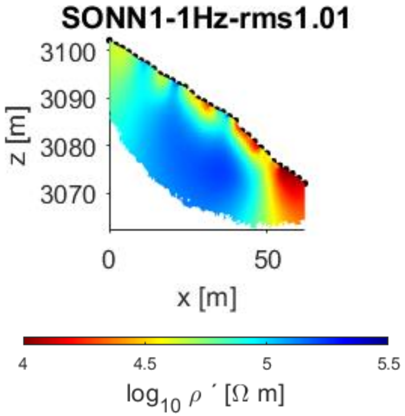

Inversion results at different frequencies - imaginary part of complex resistivity

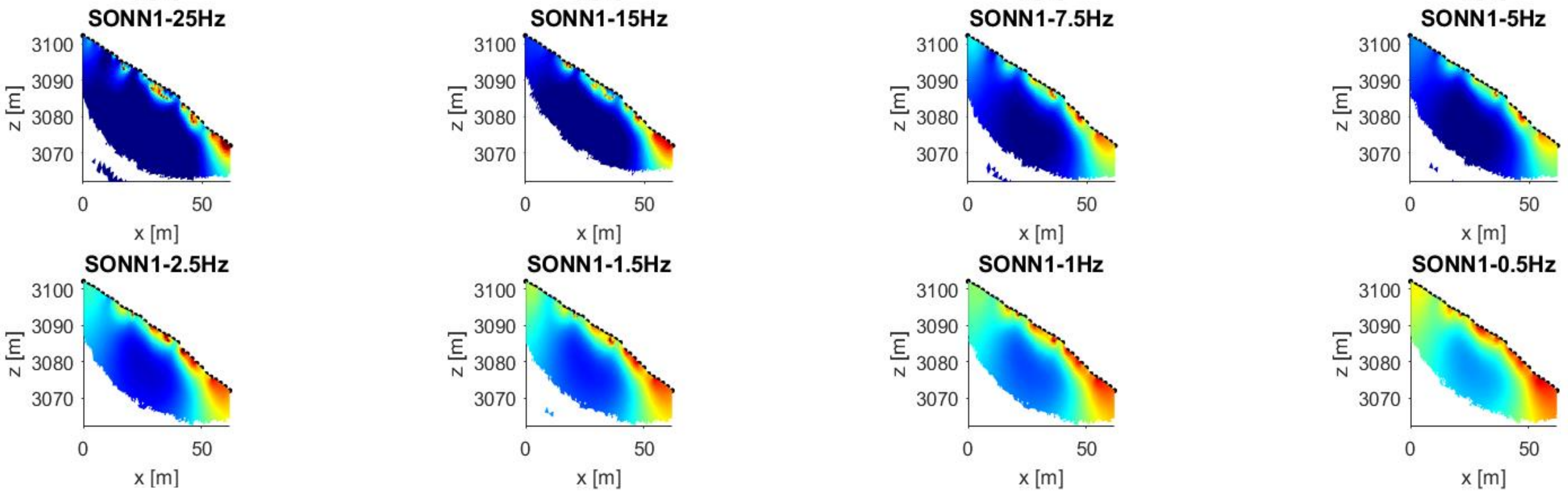

Schilthorn, Switzerland

- Schilthorn – 2970m a.s.l., Bernese Alps
- Lithology dominated by micaceous shales deeply weathered – bedrock with a layer of fine-grained debris (sandy and silty material)
- 4 boreholes (temperate permafrost)
- Permafrost thickness at least 100m, active layer depths of about 5m
- What did we measure: 1.3 km profile from permafrost to non-permafrost
- What was the aim of the study: Can we see a change in the SIP data?
- Additional information for validation: Refraction Seismic Tomography and Electromagnetic measurements

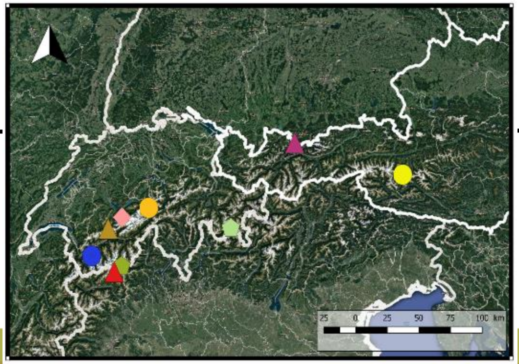

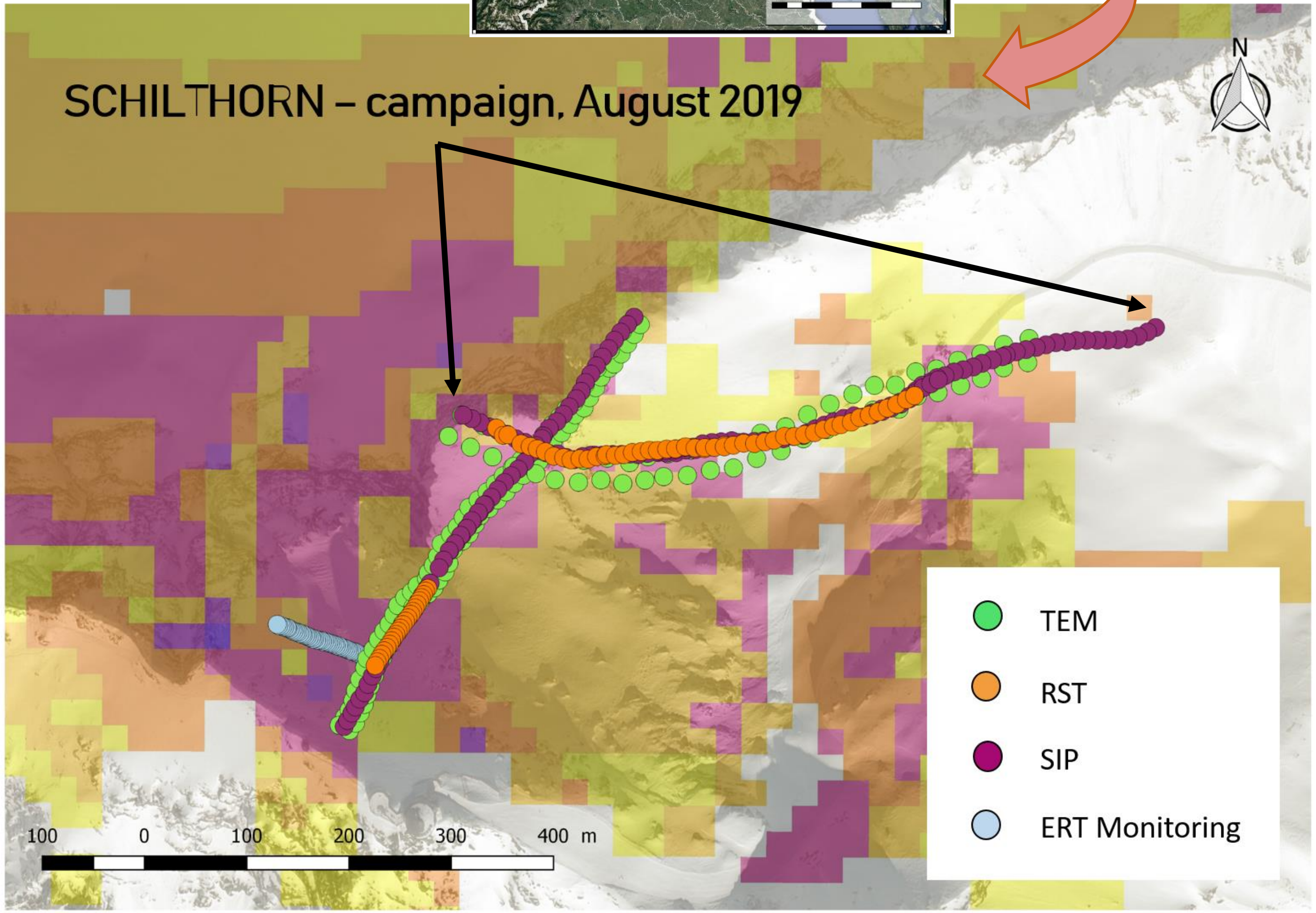

Schilthorn – long profile permafrost – no permafrost

- First SIP results for profile 2

Inversion results at different frequencies - imaginary part of complex resistivity

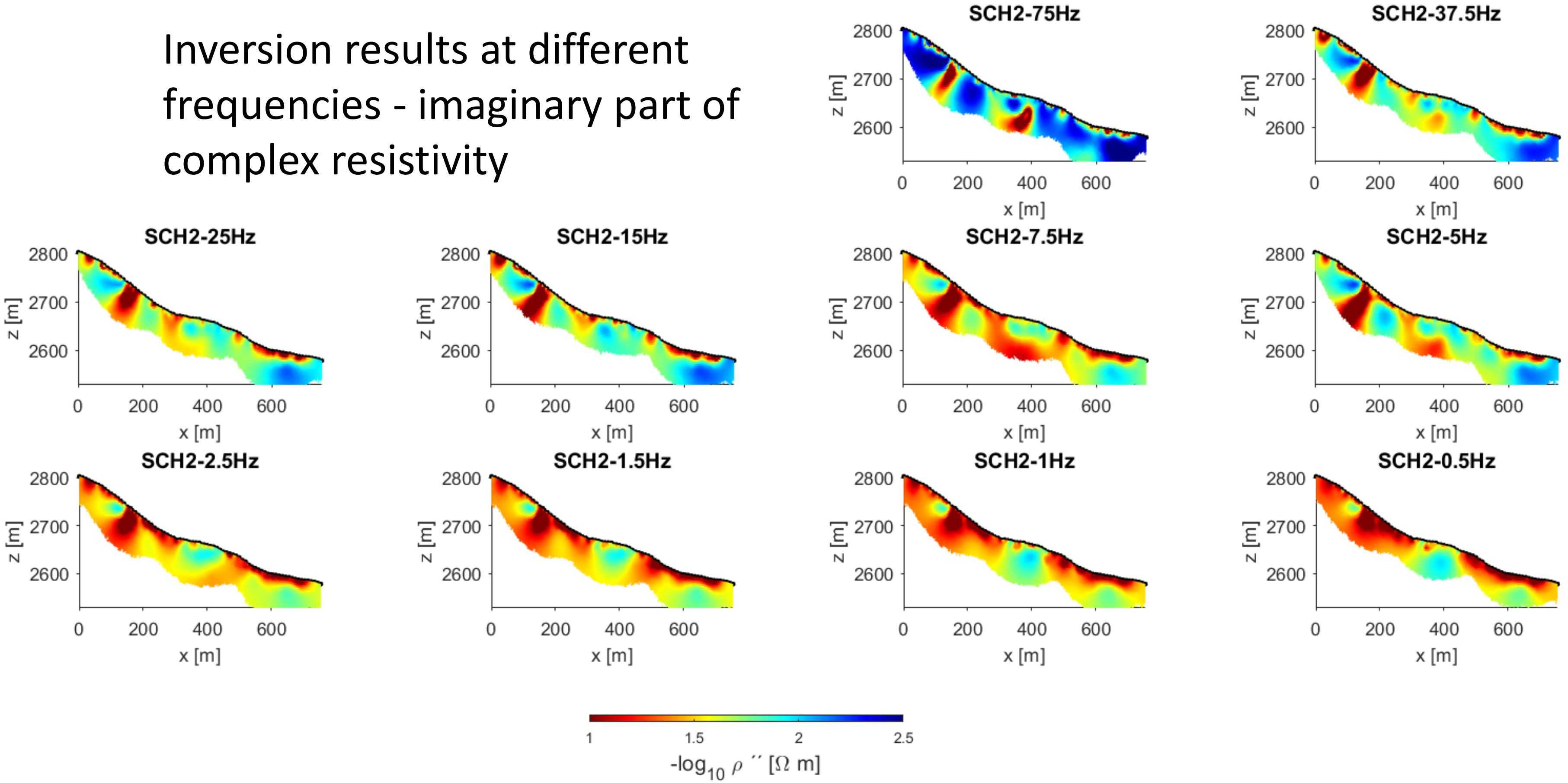

real part of complex resistivity

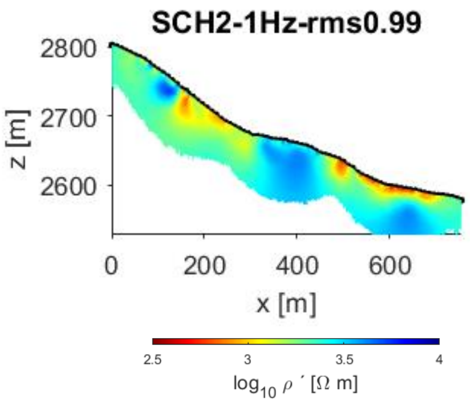

Cervinia – Italy

- Cime Bianche monitoring site
- located in the Western Alps at the head of the Valtournenche valley
- Altitude: 3100 ma.s.l.
- Homogeneous bedrock lithology mainly consisting of garnetiferous micaschists and calcschists with a cover of coarse-debris deposits (thickness ranging from few centimeters to a couple of meters)
- ALT of about 5m

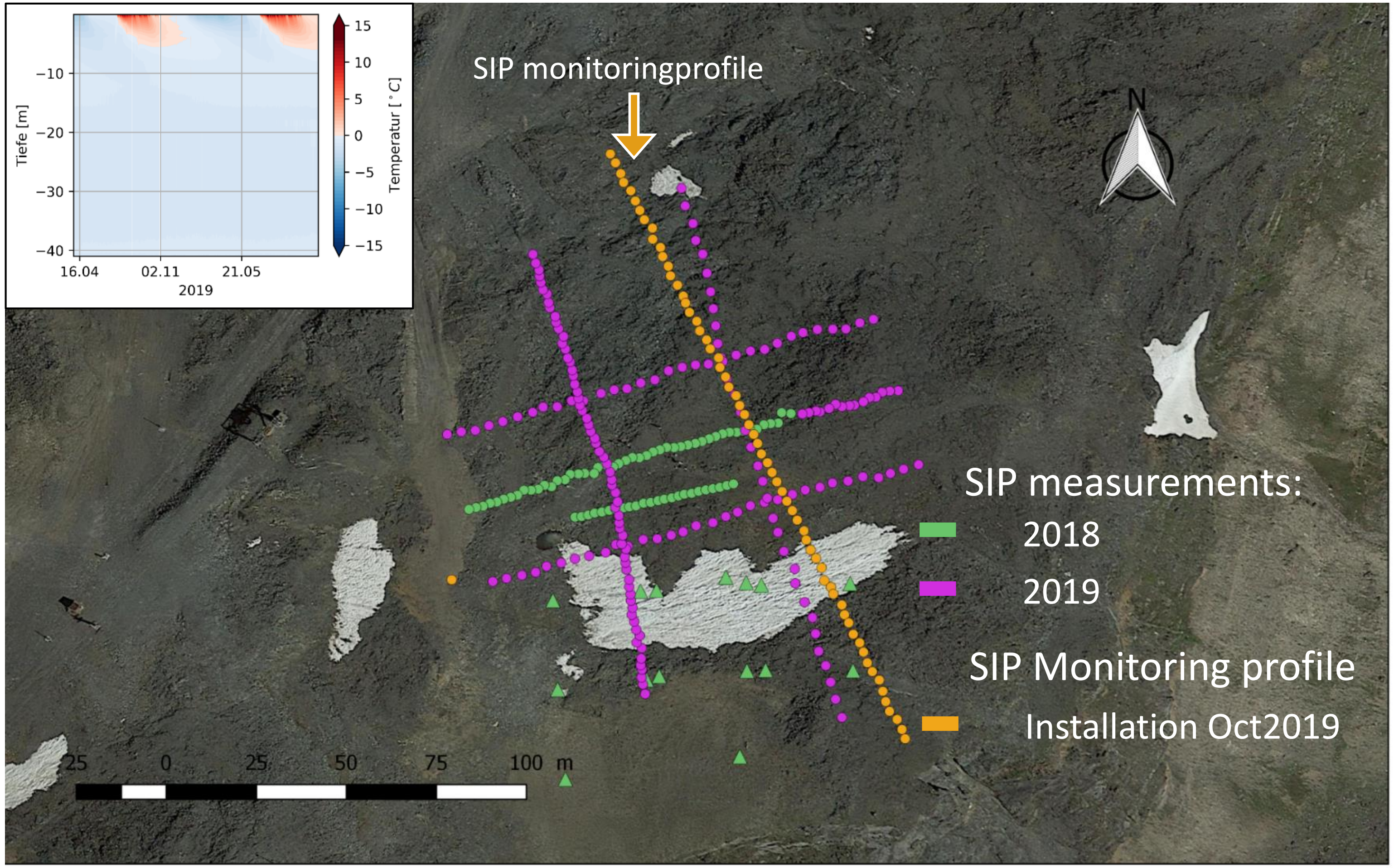

→ We chose this site as our monitoring site

Cervinia – Monitoring profile

- Complex resistivity data collected along the Monitoring profile in October 2019

Inversion results at different frequencies - imaginary part of complex resistivity

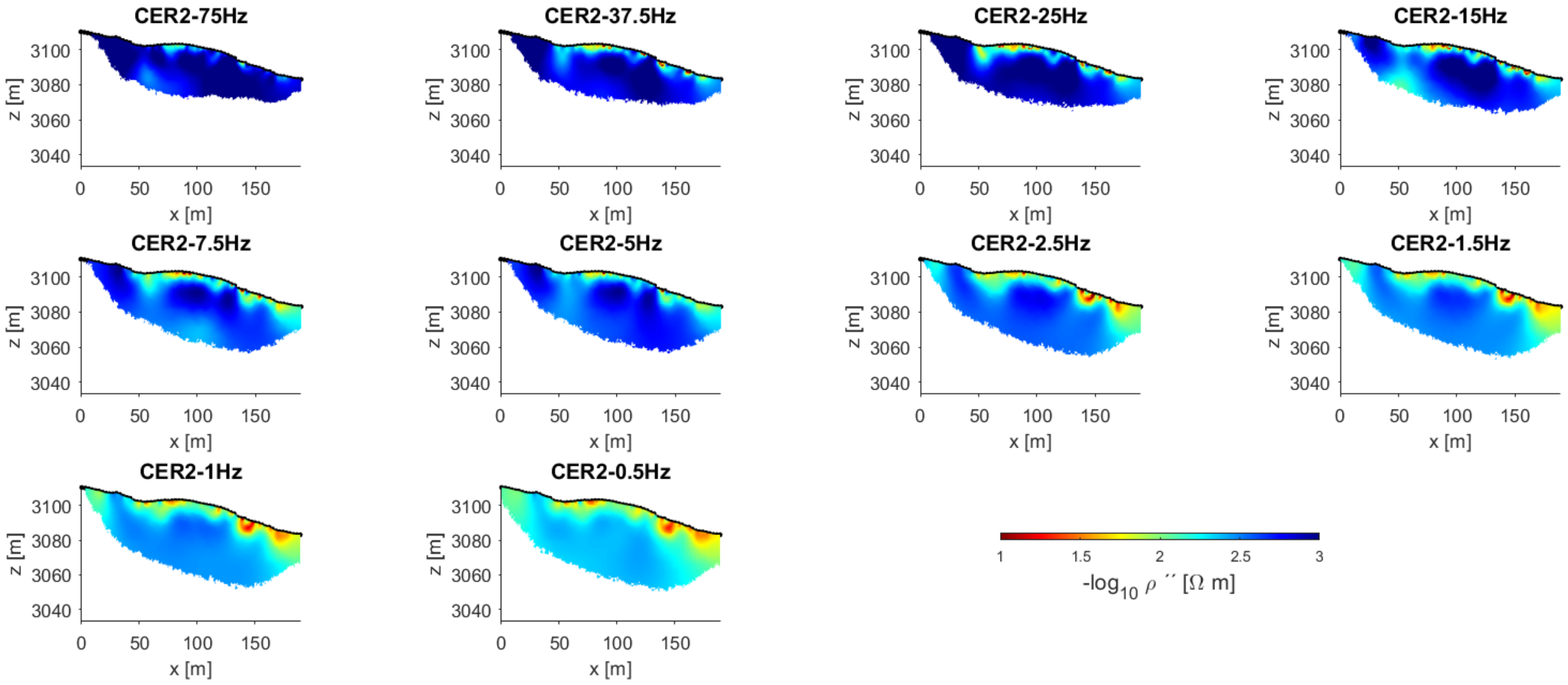

real part of complex resistivity

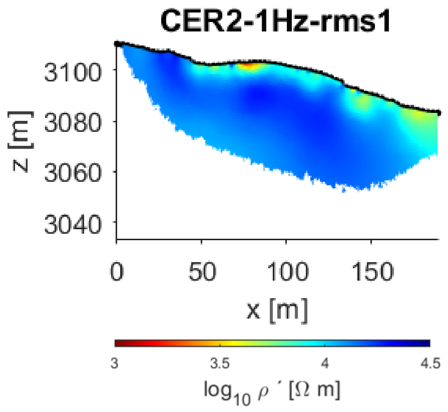

Why the low frequencies?

- Higher frequencies (>10 Hz) show a dispersion phenomenon occuring under freezing conditions which could be related to the
  - **polarization of ice**
  - superposed by the **Maxwell-Wagner** polarization mechanism

  (see Duvillard, 2018)

- At the field-scale:
  - Decreasing data quality at higher frequencies (electromagnetic coupling)

→ Comparison of different sites at lower frequencies (1 Hz)

- SIP measurements at higher frequencies– see PICO Jonas Limbrock

Complex resistivity range at different sites (1 Hz)

Schilthorn

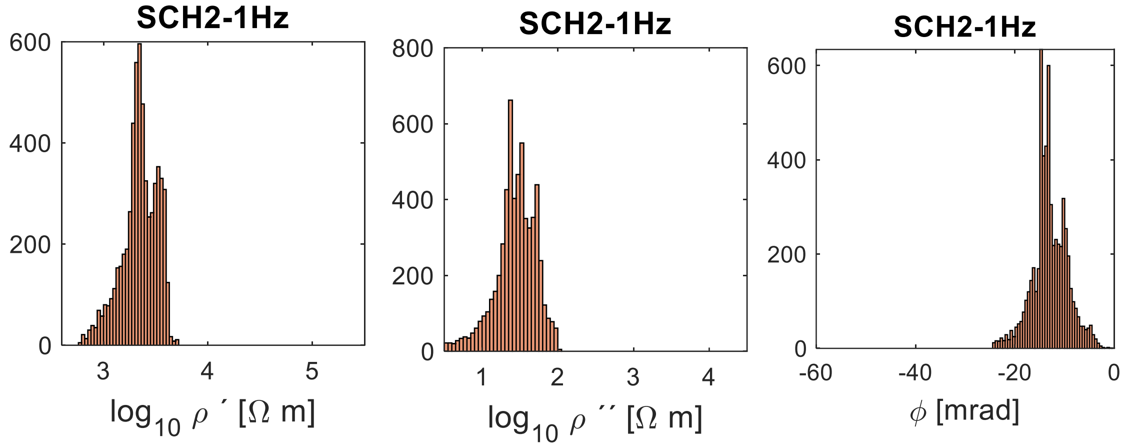

Cervinia

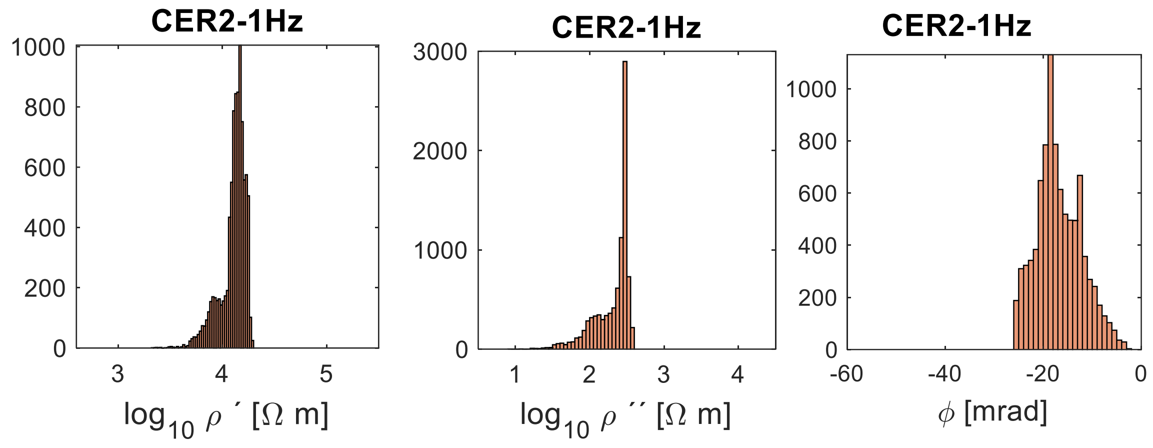

Lapires

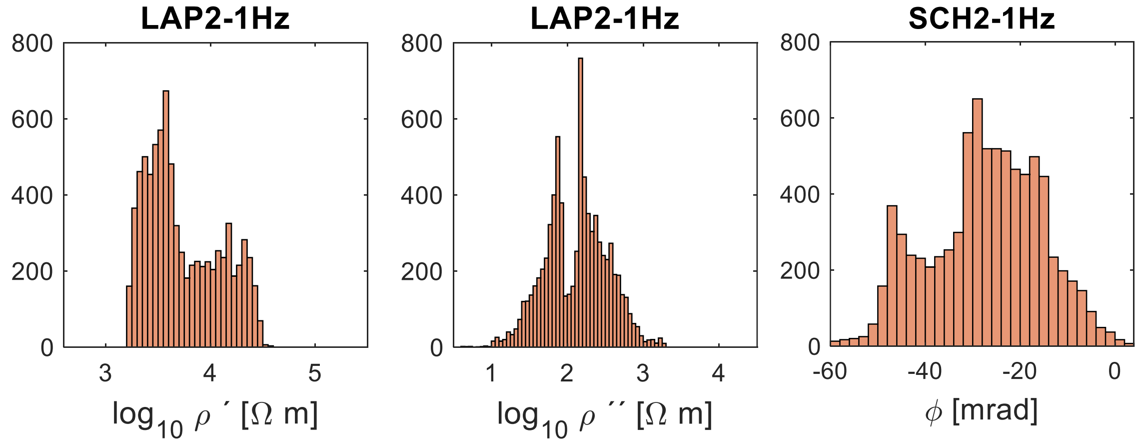

Sonnblick

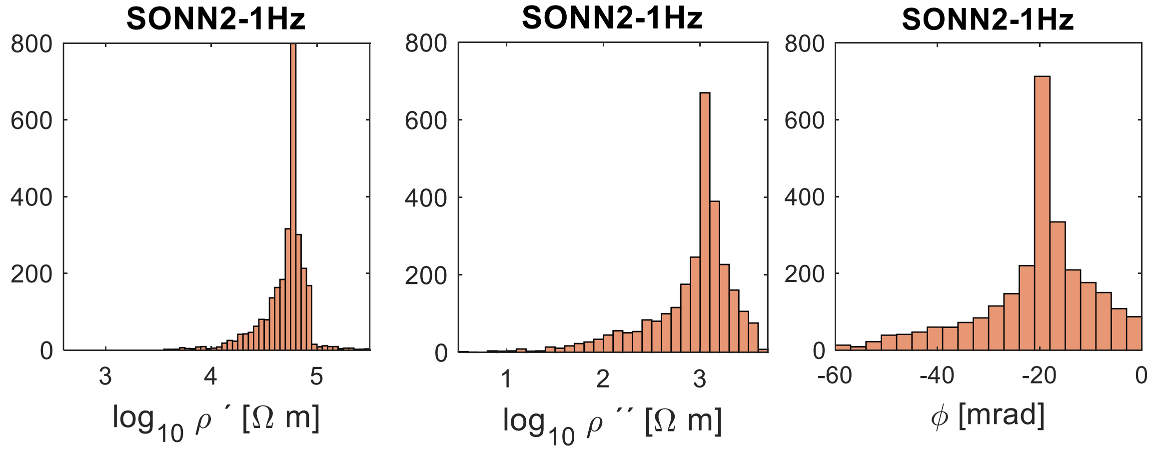

Conclusion and Outlook

- We detected a clear difference in the polarization signal between ice-rich parts and parts without ice

- We see a change in different sites showing that the complex resistivity is a good tool to characterize lithological changes and variations in ice content
- To fully understand the polarization signal for all permafrost environments – further analysis of all sites and comparison with SIP laboratory studies (Uni Bonn) necessary

- Outlook: monitoring profile Cervinia – investigation of the temporal changes in the polarization processes

- Further studies: field and laboratory studies at higher frequencies (<45 kHz) polarization of ice

→Improved thermal characterization of alpine permafrost sites by broadband SIP measurements
Jonas Limbrock, Maximilian Weigand and Andreas Kemna - D2652 | EGU2020-20081

References

- Dahlin, T., Leroux, V., & Nissen, J. (2002). Measuring techniques in induced polarisation imaging. Journal of Applied Geophysics, 50(3), 279-298.
- Delaloye, R., & Lambiel, C. (2005). Evidence of winter ascending air circulation throughout talus slopes and rock glaciers situated in the lower belt of alpine discontinuous permafrost (Swiss Alps). *Norsk Geografisk Tidsskrift-Norwegian Journal of Geography*, *59*(2), 194-203.
- Flores Orozco, A., Kemna, A., Binley, A., & Cassiani, G. (2019). Analysis of time-lapse data error in complex conductivity imaging to alleviate anthropogenic noise for site characterization. Geophysics, 84(2), B181-B193.
- Hauck, C., Bach, M., & Hilbich, C. (2008). A 4-phase model to quantify subsurface ice and water content in permafrost regions based on geophysical datasets. In *Proceedings Ninth International Conference on Permafrost, June* (pp. 675-680).
- Hilbich, C. (2010). Applicability of time-lapse refraction seismic tomography for the detection of ground ice degradation. *The Cryosphere Discussions*, *4*, 77-119.
- Kemna, A. (2000), Tomographic inversion of complex resistivity: Theory and application, Ph.D. thesis, Ruhr Univ., Bochum, Germany.
- Mollaret, C., Wagner, F. M., Hilbich, C., Scapozza, C., & Hauck, C. (2020). Petrophysical Joint Inversion Applied to Alpine Permafrost Field Sites to Image Subsurface Ice, Water, Air, and Rock Contents. *Frontiers in Earth Science*, *8*, 85.
- Mollaret, C., Hilbich, C., Pellet, C., Flores-Orozco, A., Delaloye, R., & Hauck, C. (2019). Mountain permafrost degradation documented through a network of permanent electrical resistivity tomography sites. The Cryosphere, 13(10), 2557-2578.
- Orozco, A. F., Kemna, A., & Zimmermann, E. (2012). Data error quantification in spectral induced polarization imaging. Geophysics, 77(3), E227-E237.
- Scapozza, C., Baron, L., & Lambiel, C. (2015). Borehole logging in Alpine periglacial talus slopes (Valais, Swiss Alps). *Permafrost and Periglacial Processes*, *26*(1), 67-83.
- Staub, B., Marmy, A., Hauck, C., Hilbich, C., & Delaloye, R. (2015). Ground temperature variations in a talus slope influenced by permafrost: a comparison of field observations and model simulations. Geographica Helvetica, 70(1), 45.
- Wagner, F. M., Mollaret, C., Günther, T., Uhlemann, S., Dafflon, B., Hubbard, S. S., ... & Kemna, A. (2019, January). Characterization of permafrost systems through petrophysical joint inversion of seismic and geoelectrical data. In Geophysical Research Abstracts (Vol. 21).
- Wicky, J., & Hauck, C. (2017). Numerical modelling of convective heat transport by air flow in permafrost talus slopes. The Cryosphere, 11(3), 1311-1325.